3 Biotech (2019) 9:46
https://doi.org/10.1007/s13205-019-1580-4

ORIGINAL ARTICLE

Biostimulation potentials of corn steep liquor in enhanced hydrocarbon degradation in chronically polluted soil

Lateef B. Salam[1] · **Aisha Ishaq**[1]

Received: 26 September 2018 / Accepted: 17 January 2019 / Published online: 23 January 2019

Abstract

The effects of corn steep liquor (CSL) on hydrocarbon degradation and microbial community structure and function was evaluated in field-moist soil microcosms. Chronically polluted soil treated with CSL (AB4) and an untreated control (3S) was compared over a period of 6 weeks. Gas chromatographic fingerprints of residual hydrocarbons revealed removal of 95.95% and 94.60% aliphatic and aromatic hydrocarbon fractions in AB4 system with complete disappearance of nC_1–nC_8, nC_{10}, nC_{15}, nC_{20}–nC_{23} aliphatics and aromatics such as naphthalene, acenaphthylene, fluorene, phenanthrene, pyrene, benzo(a)anthracene, and indeno(123-cd)pyrene in 42 days. In 3S system, there is removal of 61.27% and 66.58% aliphatic and aromatic fractions with complete disappearance of nC_2 and nC_{21} aliphatics and naphthalene, acenaphthylene, fluorene, phenanthrene, pyrene, and benzo(a)anthracene aromatics in 42 days. Illumina shotgun sequencing of the DNA extracted from the two systems showed the preponderance of *Actinobacteria* (31.46%) and *Proteobacteria* (38.95%) phyla in 3S and AB4 with the dominance of *Verticillium* (22.88%) and *Microbacterium* (8.16%) in 3S, and *Laceyella* (24.23%), *Methylosinus* (8.93%) and *Pedobacter* (7.73%) in AB4. Functional characterization of the metagenomic reads revealed diverse metabolic potentials and adaptive traits of the microbial communities in the two systems to various environmental stressors. It also revealed the exclusive detection of catabolic enzymes in AB4 system belonging to the aldehyde dehydrogenase superfamily. The results obtained in this study showed that CSL is a potential resource for bioremediation of hydrocarbon-polluted soils.

Keywords Corn steep liquor · Hydrocarbon-polluted soil · Soil microcosm · Illumina shotgun sequencing · Microbial community structure · Bioremediation

Introduction

Hydrocarbon pollution is a widespread problem ravaging diverse environmental matrices. While various physicochemical methods have been deployed to remediate hydrocarbon-polluted environments with relative success, the need for less destructive, environmentally friendly, cheap, technologically less demanding, green technology have attracted significant attention (Salam et al. 2015). Bioremediation, the utilization of catabolic competence of microorganisms to depurate polluted environmental compartments (Habe et al. 2001; Salam et al. 2015), is a green technology that have found applications in large scale pollution events such as the Exxon Valdez and Gulf of Mexico oil spills with outstanding successes (Pritchard et al. 1992; Fox 2011). However, there are isolated small-scale releases via indiscriminate disposal from automobile workshops, seepages from leaked pipelines and oil tankers among others that often go unnoticed and rendered hectares of arable land and aquatic environments unfit for agriculture and other activities (Obayori et al. 2015).

One of the major factors militating against efficient biodegradation of hydrocarbon pollutants even in the presence of biodegrading microorganisms is the availability of limiting nutrients. These nutrients are always limiting due to its massive demand by every member of the microbial community for various metabolic activities and other cellular processes (Andrew and Jackson 1996). In addition, such nutrients, even when present, are not bioavailable to the

Electronic supplementary material The online version of this article (https://doi.org/10.1007/s13205-019-1580-4) contains supplementary material, which is available to authorized users.

✉ Lateef B. Salam
babssalaam@yahoo.com

[1] Department of Biological Sciences, Microbiology Unit Al-Hikmah University, Ilorin, Kwara, Nigeria

biodegrading community as they readily form complexes with the hydrophobic hydrocarbons (Obayori et al. 2008, 2015). Various nutrient sources rich in macronutrients have been used as biostimulants to enhance biodegradation of hydrocarbon pollutants. These include NPK fertilizers, poultry droppings, pig dung, spent mushroom compost, natural rubber processing sludge, fish bones, cassava steep liquor, and corn steep liquor (Amadi and Bari 1992; Okolo et al. 2005; Philp et al. 2005; Yakubu 2007; Adebusoye et al. 2010; Obayori et al. 2015). With exception of NPK fertilizers that are relatively costly, these nutrient sources, which are mostly waste materials are cheap, rich in nutrients and readily available.

Corn steep liquor (CSL), a liquid mixture made of water-soluble components of corn steeped in water is a viscous liquid generated as a by-product of corn wet-milling. It is very rich in nutrients such as proteins, amino acids, carbohydrates, vitamins, and minerals required by microorganisms and is an excellent source of organic nitrogen (Liggert and Koffler 1948; Chiani et al. 2010; Saha and Racine 2010). Historically, CSL has been used as an added source of nutrient in livestock feed, fermentation processes, antibiotic production and is also a component of growth media, fertilizers and soil conditioners (Liggett and Koffler 1948; Lawford and Rousseau 1997; Filipovic et al. 2002; Obayori et al. 2010; Maddipati et al. 2011). In Nigeria, CSL is a waste liquid by-product generated from corn meal slurry production and is also used in preparations of herbal concoctions and decoctions (Obayori et al. 2010).

In hydrocarbon-polluted soils inundated with high doses of diverse classes of hydrocarbons, the microbial community structure suffered qualitatively and quantitatively. This is partly due to the varied composition and concentration of the pollutants and the differences in catabolic competence of members of the community (Bossert and Bartha 1984; Alexander 1999; Maier et al. 2000). The need to design appropriate bioremediation strategy requires adequate knowledge of the microbiota of polluted environment. The use of traditional culture-based approach though fast and cost-effective captures < 1% of the microbial community, and may give erroneous and misleading conclusions on the microbial community structure of the environment (Trevors 1998; Tabacchioni et al. 2000). The advent of culture-independent metagenomic approach particularly shotgun next generation sequencing not only provide information on the organisms present in the community but also the possible metabolic processes. Aside from the fact that this method is cheaper and enables identification of novel biomolecules with interesting functions and diverse applications (Streit and Schmitz 2004; Bashir et al. 2014), it also gives unprecedented insight into the genetic potentials of microbial communities as well as underrepresented populations (Handelsman 2004; Oulas et al. 2015).

Quantum of reports exist detailing the use of cheap nutrients to enhance the degradation of hydrocarbon pollutants in freshly polluted and chronically polluted soils (Amadi and Bari 1992; Okolo et al. 2005; Obayori et al. 2010, 2015; Adebusoye et al. 2010). However, these reports utilized culture-based approach in elucidating the microbial community involved in the degradation process. In addition, none of the existing studies elucidate the functional properties of the polluted soil prior to and after treatments with the cheap nutrient sources. Here, we report the use of a cheap nutrient source, CSL as a biostimulant to enhance the degradation of hydrocarbons in a chronically polluted soil and elucidate its effect on the microbial community structure and function.

Materials and methods

Sampling site description

Polluted soil samples were collected from an automobile workshop at Taiwo, Ilorin, Nigeria. The coordinates of the sampling site were latitude 8°28′ 42.4″N and longitude 4°32′15.6″E. The site has a long history of contamination with indiscriminately disposed spent oils spanning a period of more than 10 years.

Preparation of corn steep liquor (CSL)

Healthy maize grains (*Zea mays*) were obtained from a farm produce store in Ilorin, Nigeria. Corn steep liquor was prepared by soaking 500 g of thoroughly washed maize grains in 1 l of water for 48 h. It was thereafter grounded in a blender and left at room temperature. After another 48 h, the suspension was mixed thoroughly, strained in a domestic sieve and the liquor obtained was made up to 1 l with additional water and allowed to sediment for 2 h. The resultant supernatant was decanted, filter-sterilized using 0.22 µm membrane filter and used immediately for the bioremediation study. The physicochemistry of the CSL was determined using the methods described by Obayori et al. (2010).

Bioremediation protocols

Samples of polluted soil were collected with a sterile hand trowel after clearing the soil surface debris. The soil is dark-brown in colour, moistened with hydrocarbon mixtures with an oily odour. The soil was sieved (4 mm) and the sieved soil was thoroughly mixed in a large plastic bag to avoid variability among the results of replicate soil samples. Polluted soil (2 kg) was poured in open aluminium pans (37 cm × 14 cm × 7 cm), supplemented with 200 ml of CSL, thoroughly mixed and subsequently designated AB4. The controls designated 3S contain all materials in AB4,

but without CSL amendment. 3S was designed to determine the contribution of autochthonous microorganisms in the soil to biodegradation of the hydrocarbon pollutants. In place of CSL, the 3S soil microcosm was amended with 200 ml of sterile distilled water to maintain relatively similar moisture level with AB4. The two experimental designs AB4 and 3S were set up in triplicates and incubated at room temperature (25 ± 3 °C) for 6 weeks. Sterile distilled water (100 ml) were added to the set ups weekly to maintain moisture level of about 25%. Samples were taken at 7 days intervals for physicochemical analysis. The methods for the physicochemical analysis have been described previously (Salam et al. 2014). Residual hydrocarbons in AB4 and 3S were determined at day 0, 21 and 42 using gas chromatography.

Hydrocarbon content analysis

Polluted soil samples (10 g) were dried by mixing with 10 g anhydrous Na_2SO_4 and placed in an extraction thimble. Thereafter, 1:1 (v/v) mixture of analytical grade dichloromethane and acetone (10 ml) were added and the sample was shaken with a mechanical shaker for 30 min. The sample was collected and filtered using a glass wool plugged into a glass funnel with 1 g anhydrous Na_2SO_4 into a glass beaker. The extraction was then repeated. The extract was concentrated to 10 ml at 60 °C using rotary evaporator, after which 10 ml of hexane was added and further concentrated to about 1 ml at 60 °C. Cleanup and fractionation of the extract was done using silica gel permeation chromatography. Mixture of hexane and acetone (1:3 v/v; 10 ml) was used to extract the aliphatic fraction while 10 ml of *n*-hexane was used to extract the aromatic fraction.

Residual hydrocarbon fractions (aliphatic and aromatic) were determined by gas chromatography equipped with flame ionization detector (GC-FID). The extracts (1 µl each) were injected into GC-FID. The column OV®-3 (15-m long x 0.53 mm I.D., 0.25 µm film thickness) was used. The carrier gas is nitrogen. The injector and detector temperatures were maintained at 220 °C and 270 °C, respectively. The column was programmed at an initial oven temperature of 50 °C for 2 min; then ramped at 10°C/min to 250 °C and held for 5 min. The air flow, hydrogen flow and nitrogen flow rates are 450 ml min^{-1}, 45 ml min^{-1} and 22 ml min^{-1}, respectively.

DNA extraction, shotgun metagenomics, library construction and sequencing

Genomic DNA used for metagenomic analysis was extracted directly from the two soil microcosms AB4 and 3S. Genomic DNA was extracted from the polluted soil (3S) immediately after sampling to determine the microbial community structure and function of the polluted soil prior to CSL nutrient amendment. For the AB4 soil microcosm, genomic DNA was extracted 6 weeks after CSL fortification to determine the effects of the CSL addition on hydrocarbon degradation and microbial community structure and function. Genomic DNA were extracted from the sieved soil samples (0.25 g) using ZYMO soil DNA extraction Kit (Model D 6001, Zymo Research, USA) following the manufacturer's instructions. Genomic DNA concentration and quality was ascertained using NanoDrop spectrophotometer and electrophoresed on a 0.9% (w/v) agarose gel, respectively.

Shotgun metagenomics of 3S and AB4 microcosms was prepared using the Illumina Nextera XT sample processing kit and sequenced on a MiSEq. Genomic DNA (50 ng) were fragmented and tagmented and unique indexes were added using reduced-cycle PCR amplification consisting 8 cycles of 95 °C for 30 s, 55 °C for 30 s, and 72 °C for 30 s, and a final extension at 72 °C for 5 min before cooling to 4 °C. Constructed metagenomic libraries were purified with Agencourt AMPure XP beads and quantified with Quant-iT PicoGreen. The library size and quality were validated on Agilent Technologies 2100 Bioanalyzer. Libraries were normalized, pooled in equal volumes and run on a 600 cycles MiSeq Reagent kit v3 (Illumina Inc., San Diego, CA). All samples were multiplexed and sequenced in a single lane on the MiSeq using 2 × 300 bp paired-end sequencing, which generates 20 Mb of data for each sample. Sequence reads were generated in < 65 h, while image analysis and base calling were performed directly on MiSEq. The sequences of 3S and AB4 metagenomes were deposited on the MG-RAST server with the IDs 4704694.3 and 4704696.3 and can be accessed with the link http://www.mg-rast.org/linkin.cgi?project=mgp18598.

Sequences generated from the microcosm set up were assembled individually by VelvetOptimiser v2.2.5 and the contigs generated were fed into the MG-RAST metagenomic analysis pipeline (Keegan et al. 2016).

Taxonomic characterization of metagenomics reads and statistical analyses

The taxonomic characterization of the sequence reads of 3S and AB4 microcosms was determined using the MG-RAST server. A BLAT similarity search for the longest cluster representative in the metagenomes was performed against the MG-RAST M5rna database, which integrated SILVA, Greengenes and RDP databases. The abundance data were identified through the lowest common ancestor (LCA) with $1e^{-05}$ as the maximum *e* value, 60% as the minimum identity, and a minimum alignment length of 15 as cutoff.

Distinct taxonomic levels for each of the metagenomes retrieved from MG-RAST were statistically analyzed using the Statistical Analysis of Metagenomic Profiles, version 2 (STAMP) software (Parks et al. 2014).

In STAMP, two-sided Fisher's exact test with Newcombe–Wilson confidence interval method were used to determine the significance of the relative proportion difference in taxonomic distribution of 3S and AB4 metagenomes, while Benjamini–Hochberg FDR was applied for correction. Metagenomics reads that are unclassified were not used for analyses, and results with $q < 0.05$ were considered significant. The biological relevance of the statistic taxa was evaluated by applying a difference between the proportions of at least 1% and a twofold ratio between the proportions. In addition, various diversity indices were determined for 3S and AB4 metagenomes using MOTHUR v. 1.30.2 (Schloss et al. 2009).

Functional characterization of metagenomics reads

Gene calling was performed on the 3S and AB4 sequence reads using FragGeneScan (Rho et al. 2010) to predict open reading frames (ORFs). The ORFs were functionally annotated using the SEED subsystems annotation source of the MG-RAST, KEGG GhostKOALA, the Clusters of Orthologous Groups of proteins (COG) (Tatusov et al. 2001), and the NCBI's conserved domain database (CDD; Marchler-Bauer et al. 2015). In GhostKOALA, each query gene is assigned a taxonomic category according to the best-hit gene in the Cdhit cluster supplemented version of the non-redundant pan-genome dataset (Kanehisa et al. 2016). In addition, the ORFs were functionally annotated and assigned to the COG database that compares protein sequences encoded in complete genomes, representing major phylogenetic lineage. Sequence reads annotated for hydrocarbon degradation in 3S and AB4 metagenomes was further elucidated using the NCBI's conserved domain database (CDSEARCH/cdd v 3.15) using the default blast search parameters (*e* value 0.01).

Results

Physicochemistry of the soil microcosms and corn steep liquor

The summary of changes in physicochemistry of 3S and AB4 microcosms is depicted in Table 1. While there is a slight drop in pH from 6.76 to 6.21 in 3S, significant drop in pH from close to neutral (6.78) to acidic (5.23) was observed in AB4 at the end of 42 days. Similar trends were observed in both microcosms for phosphorus and potassium contents. However, the trends observed for these variables were much more pronounced in AB4. In contrast, at the end of 42 days, significant increase in organic matter content was observed in AB4 as compared to 3S, which only showed slight increase at days 7–21. The nitrogen contents observed in both microcosms also indicates slight increases, when compared to the initial value at day 0, though the increase is much more remarkable in AB4 microcosm. Variance analysis of the physicochemical variables of both microcosms indicates significant difference at $p < 0.05$. The physicochemistry of the CSL indicates an ash content of 16.0%, total organic carbon of 39.79%, nitrogen content of 0.18%, protein content of 1.02%, carbohydrate content of 9.6 mg/l, and phosphate content of 0.007%, respectively.

Kinetics of hydrocarbon degradation in soil microcosms 3S and AB4

The degradation of aliphatic and aromatic hydrocarbons (HC) in 3S and AB4 soil microcosms was monitored using GC/FID (Figure S1 and S2). In 3S microcosm, the residual aliphatic HC content (1332.30 mg/kg; 100%) decreased to 64.27% (856.24 mg/kg) after 21 days, corresponding to removal of 35.73% (476.05 mg/kg). Further decrease to 38.73% (515.99 mg/kg) in the residual aliphatic HC was observed at the end of 42 days, corresponding to removal of 61.27% (816.31 mg/kg) aliphatic HC. The residual

Table 1 Dynamics of physicochemical properties of polluted and CSL-amended polluted soil systems

	3S					AB4				
Time (Day)	pH	OM	P	N	K	pH	OM	P	N	K
0	6.76	1.38	6.38	0.13	0.15	6.78	1.36	6.40	0.13	0.14
7	6.79	1.35	6.31	0.13	0.15	6.80	2.62	6.48	0.12	0.16
14	6.68	1.41	6.25	0.11	0.13	6.53	2.94	6.52	0.13	0.17
21	6.63	1.42	6.00	0.14	0.16	6.18	3.23	6.40	0.17	0.19
28	6.51	1.35	6.31	0.13	0.15	5.83	3.40	6.28	0.16	0.18
35	6.30	1.34	6.30	0.12	0.15	5.65	4.41	5.61	0.15	0.18
42	6.21	1.29	6.25	0.15	0.21	5.23	4.35	5.42	0.15	0.27

OM organic matter (%), *P* available phosphorus (mg/kg), *N* total nitrogen (%), *K* potassium content (mg/kg). values are means of triplicate determinations

aromatic HC content (1325.51 mg/kg; 100%) decreased to 58.62% (777.06 mg/kg) after 21 days corresponding to the removal of 41.38% (548.45 mg/kg). The residual aromatic HC content decreased further to 33.42% (442.94 mg/kg) at the end of 42 days, corresponding to the removal of 66.58% (882.57 mg/kg) aromatic HC (Figure S1).

In AB4 microcosm, the residual aliphatic HC content (1274.09 mg/kg; 100%) decreased to 35.95% (458.08 mg/kg) after 21 days, corresponding to removal of 64.05% (816.01 mg/kg). Further decrease in the residual aliphatic HC to 4.05% (51.55 mg/kg) was observed at the end of 42 days, corresponding to the removal of 95.95% (1222.54 mg/kg) aliphatic HC. The residual aromatic HC content (1266.37 mg/kg; 100%) decreased to 32.29% (408.87 mg/kg) after 21 days corresponding to the removal of 67.71% (857.50 mg/kg). Further decrease in the residual aromatic HC content to 5.40% (68.33 mg/kg) was observed after 42 days, corresponding to the removal of 94.60% (1198.04 mg/kg) aromatic HC (Figure S2).

Significant changes in the hydrocarbon fractions in 3S and AB4 microcosms were observed during the degradation period as shown in the GC fingerprints (Figures S1 and S2; Table 2). In 3S microcosm, the GC fingerprints of the aliphatic fractions showed complete disappearance of nC_2 ethane and nC_{21} heneicosane fractions at the end of 42 days. Significant reductions to < 30% were also observed for nC_1 methane, nC_4 methylpropane, nC_5 methylbutane, nC_{11} undecane, nC_{15} pentadecane, nC_{19} nonadecane, nC_{20} eicosane, nC_{22} docosane, and nC_{23} tricosane, respectively. The GC fingerprints of the aromatic fractions showed complete disappearance of naphthalene, acenaphthylene, fluorene, phenanthrene, pyrene, and benzo(a)anthracene at the end of 42 days, while significant reduction to < 25% were observed for fluoranthene and indeno(123-cd)pyrene, respectively (Figure S1, Table 2).

In AB4 microcosm, the GC fingerprints of the aliphatic fractions showed complete disappearance of nC_1 methane, nC_2 ethane, nC_3 propane, nC_3 cyclopropane, nC_4 butane, nC_4 methylpropane, nC_5 pentane, nC_5 methylbutane, nC_6 hexane, nC_8 octane, nC_8 2,2,4-trimethylpentane, nC_{10} decane, nC_{15} pentadecane, nC_{20} eicosane, nC_{21} heneicosane, nC_{22} docosane and nC_{23} tricosane at the end of 42 days. Significant reduction to < 10% were also observed for nC_9 nonane, nC_{11} undecane, nC_{12} dodecane, nC_{17} heptadecane, phytane and nC_{19} nonadecane fractions. The GC fingerprints of the aromatic fractions showed complete disappearance of naphthalene, acenaphthylene, fluorene, phenanthrene, pyrene, benzo(a)anthracene and indeno(123-cd)pyrene at the end of 42 days, while significant reduction of < 10% (with exception of acenaphthene and anthracene) were observed for the other polyaromatics (Figure S2, Table 2).

General characteristics of the metagenomes

Illumina miseq sequencing of the two hydrocarbon-polluted soil microcosms resulted in 1,239 and 694 sequence reads for 3S and AB4 with a total of 314,848 and 170,673 bp, an average length of 254 ± 66 and 246 ± 66 bp, and the mean GC content of 61 ± 6 and 59 ± 6%, respectively. After denoising and normalization by DynamicTrim (Cox et al. 2010), and removal of sequencing artefacts and host DNA contamination removal by Bowtie-2 using default parameters (Langmead and Salzberg 2012), the sequence reads in 3S and AB4 reduced to 1,064 and 612 with a total of 260,627 and 147,225 bp and an average sequence length of 245 ± 55 and 241 ± 58 bp, respectively. Statistical analyses of the species richness and abundance in the 3S and AB4 metagenome revealed 939 and 528 unique phylotypes at species delineation (0.03, 97%) as shown in the rarefaction curve (Fig. 1). In addition, the analysis revealed that Shannon index (*H'*) was 8.57 and 7.92; Simpson's index (*D*) was 0.000455 and 0.000648; Simpson's reciprocal index (1/*D*) was 2200 and 1543; and Chao index was 10855.92 and 4642.34, respectively.

Comparative structural diversity of the metagenomes

Comparative analysis of the microbial community structure of the two metagenomes, 3S and AB4 revealed significant differences in the taxonomic profiles generated by MG-RAST. In phylum classification, the predominant phyla in 3S microcosm are *Actinobacteria* (31.46%), *Ascomycota* (22.52%), *Proteobacteria* (19.52%), and *Firmicutes* (17.71%). In contrast, the predominant phyla in CSL-amended AB4 microcosm are *Proteobacteria* (38.95%), *Firmicutes* (28.30%), *Bacteroidetes* (15.58%), and *Actinobacteria* (10.33%), respectively. Representative phyla belonging to *Archaea* domain were not recovered from AB4 microcosm while sequences belonging to viruses, which cannot be placed in any of the existing phyla, were also recovered from AB4 microcosm (Fig. 2).

In class delineation, the predominant classes in 3S microcosm are *Actinobacteria* (31.98%), *Sordariomycetes* (22.83%), *Clostridia* (10.43%), *Alphaproteobacteria* (9.51%), and *Gammaproteobacteria* (6.01%), while *Bacilli* (25.61%), *Alphaproteobacteria* (23.82%), *Sphingobacteriia* (10.86%), *Actinobacteria* (10.53%), and *Gammaproteobacteria* (10.21%) are preponderant in AB4 microcosm (Fig. 3).

In order delineation, *Actinomycetales* (31.22%) and *Bacillales* (25.04%) are the predominant orders in 3S and AB4 microcosms. Aside from the predominant orders, other orders with the highest representation include *Glomerellales* (23.13%), *Clostridiales* and *Bacillales* in 3S microcosm and *Rhizobiales* (13.12%), *Sphingobacteriales* (11.41%),

Table 2 Percentage representative residual aliphatic and aromatic hydrocarbons in 3S and AB4 polluted systems after 21 and 42 days of incubation at room temperature

Hydrocarbon fractions	3S Microcosm			AB4 Microcosm		
	Day 0	Day 21	Day 42	Day 0	Day 21	Day 42
Aliphatics						
nC_1 methane	100	43.56	25.35	100	44.34	0.00
nC_2 ethane	100	56.62	0.00	100	59.63	0.00
nC_3 propane	100	72.75	40.02	100	45.27	0.00
nC_3 cyclopropane	100	79.31	43.33	100	41.66	0.00
nC_4 butane	100	73.37	33.19	100	30.80	0.00
nC_4 methylpropane	100	70.08	16.86	100	24.48	0.00
nC_5 pentane	100	80.65	53.90	100	37.84	0.00
nC_5 methylbutane	100	67.89	16.19	100	11.90	0.00
nC_6 hexane	100	83.66	55.26	100	52.71	0.00
nC_7 heptane	100	73.25	35.05	100	28.55	36.70
nC_8 octane	100	83.02	60.72	100	48.68	0.00
nC_8 2,2,4-trimethylpentane	100	85.86	64.93	100	63.85	0.00
nC_9 nonane	100	75.61	34.80	100	31.31	9.76
nC_{10} decane	100	81.69	53.11	100	42.79	0.00
nC_{11} undecane	100	65.30	24.40	100	23.20	7.20
nC_{12} dodecane	100	72.64	49.24	100	51.00	8.88
nC_{13} tridecane	100	61.88	31.74	100	11.64	19.94
nC_{14} tetradecane	100	77.69	54.93	100	57.09	11.36
nC_{15} pentadecane	100	50.77	17.71	100	0.00	0.00
nC_{16} hexadecane	100	71.48	51.07	100	46.36	14.11
nC_{17} heptadecane	100	69.44	46.82	100	39.83	9.04
Pristane	100	66.61	43.32	100	33.56	15.74
nC_{18} octadecane	100	67.69	42.11	100	37.96	16.75
Phytane	100	65.28	37.46	100	39.02	2.96
nC_{19} nonadecane	100	52.50	23.20	100	23.42	2.44
nC_{20} eicosane	100	48.77	24.61	100	29.86	0.00
nC_{21} heneicosane	100	24.30	0.00	100	0.00	0.00
nC_{22} docosane	100	31.71	12.08	100	17.60	0.00
nC_{23} tricosane	100	15.97	11.77	100	9.45	0.00
Aromatics						
Naphthalene	100	0.00	0.00	100	0.00	0.00
Acenaphthylene	100	82.28	0.00	100	76.00	0.00
Acenaphthene	100	72.80	40.46	100	61.62	32.39
Fluorene	100	77.24	0.00	100	67.90	0.00
Phenanthrene	100	64.91	0.00	100	53.06	0.00
Anthracene	100	56.97	40.31	100	46.52	14.96
Fluoranthene	100	76.06	23.59	100	71.69	7.80
Pyrene	100	66.97	0.00	100	45.30	0.00
Benzo(a)anthracene	100	59.52	0.00	100	32.19	0.00
Chrysene	100	50.36	53.49	100	28.83	8.65
Benzo(b)fluoranthene	100	54.33	60.99	100	24.76	5.73
Benzo(a)pyrene	100	62.90	42.67	100	26.09	1.58
Dibenzo(a,h)anthracene	100	64.64	43.01	100	25.85	1.86
Benzo(ghi)perylene	100	46.73	51.01	100	6.57	1.45
Indono(123-cd)pyrene	100	45.11	18.87	100	25.00	0.00

Values were calculated from peak areas on day 21 and day 42, respectively, relative to peak area values for day 0

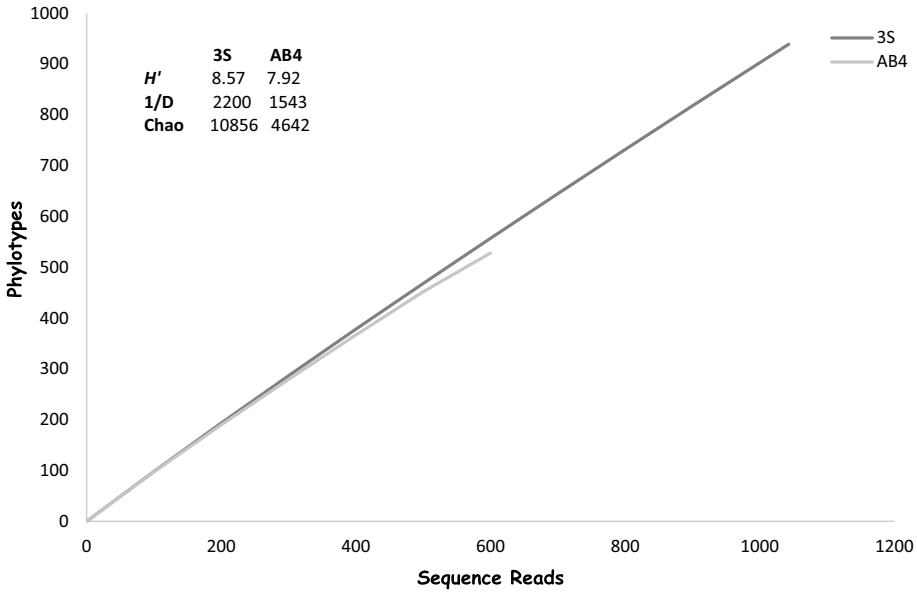

Fig. 1 Rarefaction curve of number of unique sequences (phylotypes) recovered vs. number of sequence reads for 3S and AB4 metagenomes. The phylotypes (OTUs) are 939 and 528 for 3S and AB4 at species delineation (0.03, 97%)

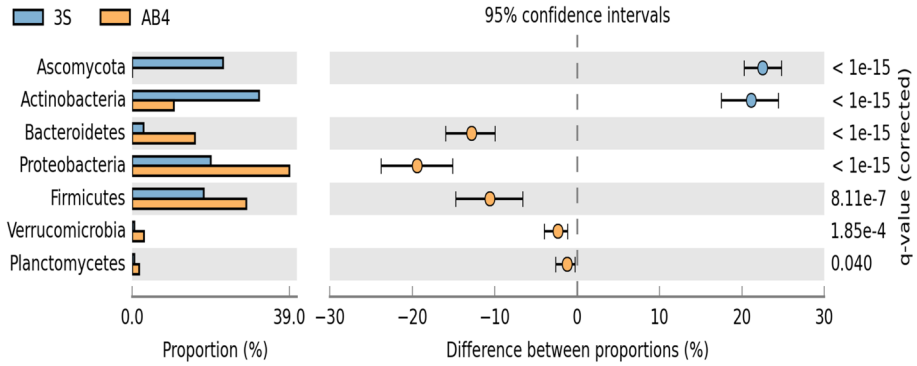

Fig. 2 Comparative taxonomic profile of the 3S and AB4 microcosms at phylum level, computed by MG-RAST. Only phyla with significant biological differences ($P < 0.05$, difference between the proportions > 1% and twofold of ratio between the proportions, as determined by STAMP) are shown and metagenomic reads that are unclassified were not used for analyses

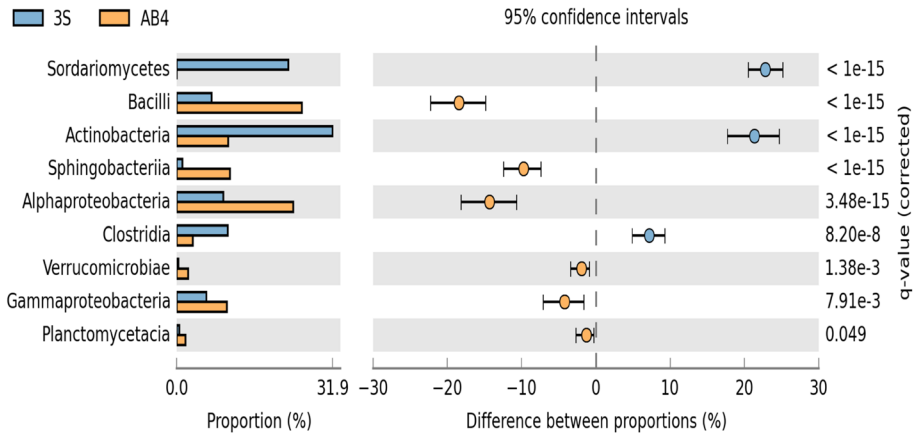

Fig. 3 Comparative taxonomic profile of the 3S and AB4 microcosms at class level, computed by MG-RAST. Only classes with significant biological differences ($P < 0.05$, difference between the proportions > 1% and twofold of ratio between the proportions, as determined by STAMP) are shown and metagenomic reads that are unclassified were not used for analyses

and *Actinomycetales* (10.73%) in AB4 microcosm (Figure S3). In family classification, the 3S microcosm showed the preponderance of *Plectosphaerellaceae* (23.38%), *Microbacteriaceae* (9.59%), *Syntrophomonadaceae* (7.17%), and *Brevibacteriaceae* (5.46%) while *Thermoactinomycetaceae* (25.00%), *Methylocystaceae* (9.40%), *Sphingobacteriaceae* (9.04%), and *Caulobacteraceae* (4.43%) are predominant in AB4 microcosm, respectively (Figure S4).

The genus delineation of the two microcosms presents interesting findings. In 3S microcosm, the predominant

genus is *Verticillium* (22.88%), a representative of the phylum *Ascomycota*. Other genera with significant representation include *Microbacterium* (8.16%), *Dethiobacter* (6.94%), *Brevibacterium* (5.34%), and *Pseudomonas* (3.36%). In AB4 microcosm, the genus with the highest abundance is *Laceyella* (24.23%), a representative of the phylum *Firmicutes*. Other predominant genera include *Methylosinus* (8.93%), *Pedobacter* (7.73%), *Terrimonas* (2.58%), *Brevundimonas* (2.06%), and *Xanthomonas* (1.89%), respectively (Fig. 4).

Comparative functional diversity of the metagenomes

Comparative analysis of the functional diversity of the two microcosms using the MG-RAST SEED subsystem revealed the abundance of clustering-based subsystems (which group hypothetical protein families based on conserved co-localization across multiple genomes) (17.65%), miscellaneous (14.71%), carbohydrate (9.80%) and amino acid and derivatives (8.82%) subsystems in 3S microcosm. In CSL-treated AB4 microcosm, clustering-based subsystems (27.08%), miscellaneous (4.90%), membrane transport (4.90%), and protein metabolism are preponderant. In addition, aside from metabolism of aromatic compounds (3S 2.84%; AB4 2.98%), which were detected in the two microcosms, other important subsystems such as stress response (1.96%), phages, prophages, transposable elements, plasmids (3.92%) and motility and chemotaxis (0.98%) that were conspicuously absent in AB4 were present in 3S microcosm (Fig. 5).

Elucidation of the metabolic properties of the two microcosms using KEGG GhostKOALA also revealed the presence of efflux systems and heavy metal resistance genes responsible for resistance, transport, and detoxification of heavy metals as well as transport of inorganic nutrients such as nitrogen, phosphorus, sulfur, among others (Tables 3, 4). Furthermore, as shown in Tables 3 and 4, comparison of annotated genes recovered in 3S and AB4 microcosms for transport of inorganic nutrients, heavy metal transport, resistance and detoxification revealed significant differences. Detected genes are higher in 3S than in AB4. In addition, genes for potassium metabolism not detected in 3S were detected in AB4, while genes for nickel transport detected in 3S were absent in AB4. Moreover, taxonomic classification of annotated genes from the two microcosms also revealed significant differences as shown in Tables 3 and 4.

The NCBI's CDD was used to further elucidate sequence reads in the two metagenomes previously annotated for hydrocarbon degradation in MG-RAST and COG databases. As shown in Tables 5 and 6, majority of the genes code for enzymes involved in aerobic degradation of polycyclic and heterocyclic aromatic hydrocarbons. In 3S microcosm, aromatic degrading enzymes recovered include enzymes of the Rieske non-haem iron oxygenase family such as vanillate *O*-demethylase oxygenase subunit, dicamba *O*-demethylase oxygenase, phenylpropionate dioxygenase, biphenyl dioxygenase and carbazole 1,9a-dioxygenase; and FAA hydrolase enzymes involved in catechol pathway and 4-hydroxyphenylacetate degradation. Others include short-chain dehydrogenase/reductase (SDR) enzymes involved in conversion of 1,2-dihydroxycyclohexa-3,4-diene carboxylate to a catechol and biphenyl/polychlorinated biphenyl degradation; enzymes involved in anaerobic degradation of benzoate; dibenzothiophene desulfurization enzyme C; various transcriptional regulators, and several others (Table 5). In AB4 microcosm, aside from the detection of Rieske non-heme iron oxygenases not detected in 3S such as anthranilate 1,2-dioxygenase, phthalate 4,5-dioxygenase, and 2-oxoquinoline 8-monooxygenase, various enzymes of the aldehyde dehydrogenase family were also detected. These include

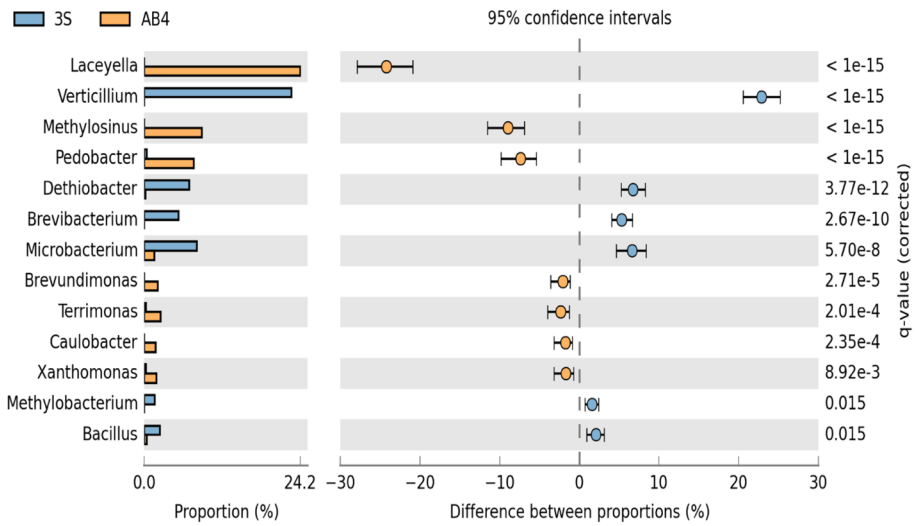

Fig. 4 Comparative taxonomic profile of the 3S and AB4 microcosms at genus level, computed by MG-RAST. Only genera with significant biological differences ($P < 0.05$, difference between the proportions > 1% and twofold of ratio between the proportions, as determined by STAMP) are shown and metagenomic reads that are unclassified were not used for analyses

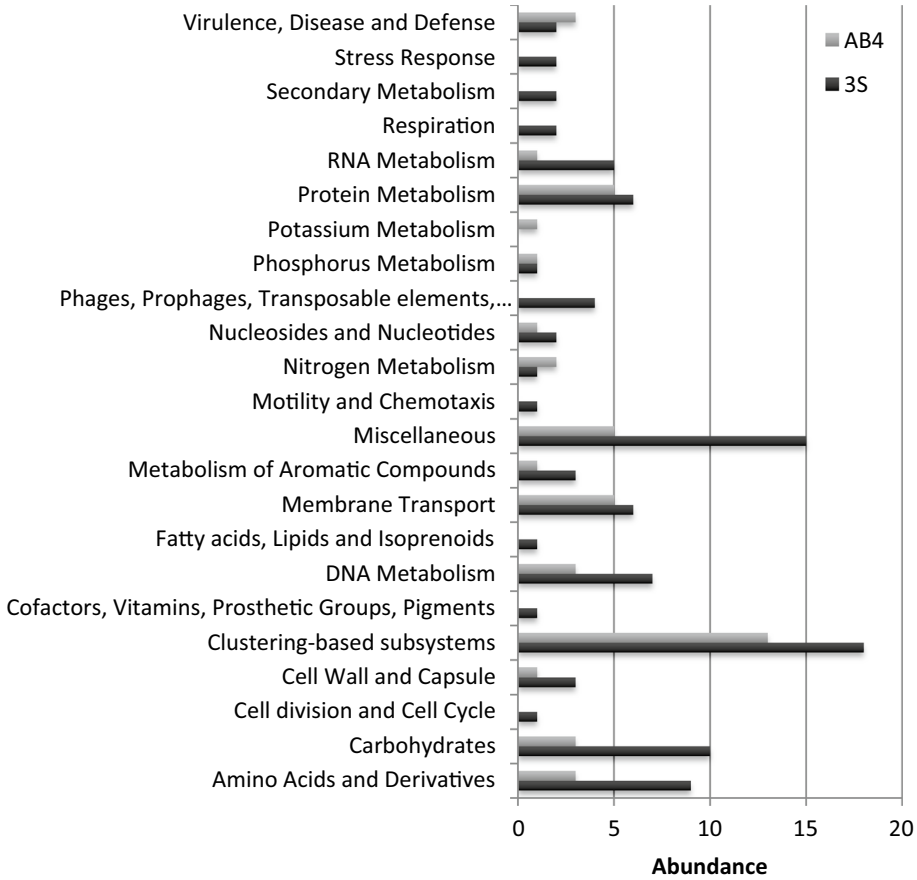

Fig. 5 Comparative functional profile of 3S (in black) and AB1 (in grey) microcosms identified by MG-RAST using the SEED subsystem

aldehyde dehydrogenase, vanillin dehydrogenase, salicylaldehyde dehydrogenase, 2- and 4-hydroxymuconic semialdehyde dehydrogenase, *p*-hydroxybenzaldehyde dehydrogenase among others. These enzymes are involved in biocatalysis of diverse aromatic and polyaromatic hydrocarbons and several others indicated in Table 6.

Functional profile of the sequence reads of the two metagenomes, 3S and AB4 were further analyzed by assigning predicted functions to genes based on COG. For 3S and AB4 microcosms, 20 classes based on functional categories were identified by the COG database (Fig. 6). In 3S microcosm, classes with highest representation in 3S microcosm are "carbohydrate transport and metabolism (G)", "inorganic ion transport and metabolism (P)", and "amino acid transport and metabolism (E)", respectively. However, in AB4 microcosm, classes with highest representation are "amino acid transport and metabolism (E)", "inorganic ion transport and metabolism (P)", and "carbohydrate transport and metabolism (G)". hydrocarbon degradation genes such as Rieske non-heme oxygenases, 2-keto-4-pentenoate hydratase/2-oxohepta-3-ene-1,7-dioic acid hydratase (catechol pathway) and several others were detected in the class "secondary metabolites biosynthesis, transport and catabolism (Q)" in the two metagenomes (Fig. 6).

Discussion

Contamination of the environment with petroleum hydrocarbons and other toxic and hazardous chemicals are considered the most frequent organic pollutants of soil and water ecosystems. It is a persistent and widespread pollution problem and the recalcitrant, toxic, and mutagenic properties of its constituents imposes significant health implications and ecological disturbances (Bundy et al. 2002; Okoh 2006; Salam et al. 2018). Of paramount interest is the need to design an effective bioremediation strategy for sites polluted with these hydrocarbons. An increasingly adopted strategy is biostimulation, an in situ bioremediation strategy that enhance the biodegradative capacity of indigenous microbial community in soil via stimulation by addition of limiting nutrients, water and oxygen. The success of this strategy is predicated on the presence of sizeable population of biodegrading microorganisms that harbours diverse catabolic genes and enzymes required for degradation of the pollutants in such systems. In this study, we have shown that the use of CSL can effectively enhance bioremediation of hydrocarbon-polluted soil.

While the toxicity of various constituents of hydrocarbons to microbial communities in hydrocarbon-polluted soils may account for slow pollutants removal (Teal et al. 1992; Yveline et al. 1997), several authors have also attributed this

Table 3 List of the enzymes/genes identified in 3S polluted system involved in heavy metal resistance and transport/regulation of macronutrients and their taxonomic affiliations

Macronutrients	Enzymes/genes	Microorganisms
Sulfur	Sulfite reductase (NADPH) beta subunit (hemoprotein); sulfate permease and related transporters (MFS superfamily); GTPases-sulfate adenylate transferase subunit 1; bifunctional sulfate adenylyltransferase subunit 1/adenylylsulfate kinase protein; taurine transporter subunit 1; Alkanesulfonate transporter substrate-binding subunit; Anaerobic sulfite reductase subunit B; sulfate transport system, permease protein; sulfonate transport system substrate binding protein; CysN/CysC bifunctional enzyme, ATP-sulfurylase lage subunit and adenylyl sulfate kinase; ABC CysA domain of the sulfate transporter; aliphatic sulfonate transport, ATP-binding subunit; C-terminal substrate binding domain of LysR transcriptional regulator, CysL; alkanesulfonate monooxygenase; sulfate/thiosulfate transporter	*Ensifer, Alkalilimnicola, Chelatococcus, Comamonadaceae bacterium A1, Pseudomonas, Starkeya, Dokdonella, Stenotrophomonas, Pelagibaca, Rubrobacter*
Nitrogen	Ferredoxin nitrite reductase; nitrite reductase (NADH) small subunit; glutamate synthase (NADPH/NADH) large chain; ABC domain of nitrate and sulfonate transporters; nitrate transport ATP-binding subunit; signal transduction histidine kinase involved in nitrogen fixation and metabolism regulation; nitrate/nitrite sensor protein, NarX; C-terminal substrate binding domain of LysR nitrogen assimilation control (NAC)	*Ensifer, Sphingopyxis, Methylobacterium, Achromobacter, Stenotrophomonas, Pelagibaca, Blastococcus*
Phosphorus	Polyphosphate kinase; ABC-type phosphonate transport system, ATPase component; phosphonate C-P lyase system protein PhnK; PTS-HPR, phosphocarrier protein; inorganic phosphate transporter, PiT family; ABC domain of the phosphate transport system, PstB subunit; phosphonate ABC transporter; phosphonate/organophosphate ester transporter subunit; phosphonate C-P lyase system protein PhnL	*Thermovibrio, Roseomonas, Achromobacter, Cutibacterium, Luteibacter, Stenotrophomonas, Pelagibaca*
Sodium, magnesium and multiple Cations transport	Mg^{2+} and Co^{2+} transporter, CorB; magnesium transporter, CorA; NatA, ATpase component of bacterial ABC-type Na^{+} transport system; solute carrier family 10 (sodium/bile acid co-transporter), member 7; phosphate/sulfate permeases; ABC-type nitrate/sulfonate/bicarbonate transport system, permease component; ABC-type nitrate/sulfonate/bicarbonate transport system, periplasmic components; cation transport ATPase	*Stenotrophomonas, Pseudomonas, Pelagibaca, Oceanimonas, Luteibacter, Comamonadaceae bacterium A1, Micrococcus, Sphingomonas*
Metal resistance/transport genes		
Iron	ABC-type Fe^{3+} transport system, permease component; outer membrane receptor proteins, mostly Fe transport; ABC-type Fe^{2+}-enterobactin transport system, periplasmic component; iron-hydroxamate transporter, ATP-binding subunit; ABC-type iron transport system, FetAB, ATPase component; ABC-type enterochelin transport system, ATPase component; ABC-type siderophore export system, fused ATPase and permease components	*Ochrobactrum, Pseudomonas, Rhodovulum, Pelagibaca*

Table 3 (continued)

Macronutrients	Enzymes/genes	Microorganisms
Nickel	ABC-type dipeptide/oligopeptide/nickel transport system, permease components; nickel import ATP-binding protein, NikE subunit; NikD, nickel import ATP-binding protein	*Pseudothermotoga, Catenulispora, Brachybacterium, Pelagibaca, Stenotrophomonas*
Cobalt, cadmium, lead, zinc, mercury	Zinc/cadmium/mecury/lead transporting ATPase; cobalt-zinc-cadmium resistance protein, CzcA; Cd^{2+}/Zn^{2+}-exporting ATPase; Domain I of the ABC component of cobalt transport system; domain II of the ABC component of cobalt transport family, CbiO protein; high-affinity zinc transporter ATPase; Helix-Turn-Helix (HTH) DNA binding domain of CadR and PbrR transcription regulators; Cd(II)/Pb(II)-responsive transcriptional activator of the proteobacterial metal efflux system; HTH DNA binding domain of the heavy metal resistance transcription regulators (MerR1, CueR, CadR, PbrR, ZntR and other related protein); CueR and ActP HTH transcription regulator; MerR1 HTH transcriptional regulator	*Micrococcus, Sphingomonas, Achromobacter, Stenotrophomonas, Pelagibaca, Sphingobium*
Manganese, molybdenum, silver, copper	Mn^{2+}/Fe^{2+} transporters of the NRAMP family; putative silver efflux pump; manganese transport protein (MntH); Cu^{+}-exporting ATPase, CopA ATP7; Cu^{2+}-exporting ATPase, CopB; ABC domain of molybdenum transport system, ModC; ABC-type molybdenum transport system. ATPase component/photorepair protein PhrA	*Pseudomonas geniculata, Microbacterium, Candidatus solibacter, Nitrobacter, Achromobacter, Propionibacterium, Confluentimicrobium, Stenotrophomonas, Pelagibaca*

Table 4 List of the Enzymes/genes identified in AB4 polluted system involved in heavy metal resistance and transport/regulation of macronutrients and their taxonomic affiliations

Macronutrients	Enzymes/genes	Microorganisms
Sulfur	Sulfate permease and related transporters (MFS superfamily); arylsulfatase A and related enzymes; sulfate/thiosulfate transporter subunit; alkanesulfonate transporter, permease subunit; sulfonate transport system	*Xanthomonas, Roseomonas, Zhongshania, Polyangium brachysporum*
Nitrogen and potassium	NAD(P)H-nitrite reductase, ferredoxin subunits of nitrite reductase and ring hydroxylating enzymes; glutamate synthase (NADPH/NADH) large chain; Kef-type K^+ transport system, membrane component; glutathione-regulated potassium efflux system protein KefC	*Sphingopyxis, Pseudomonas geniculata, Paracoccus*
Phosphorus and multiple cations transport	Cation transport ATPase, two-component system OmpR family, response regulator PhoP; two component system, OmpR family, phosphate regulon sensor histidine kinase PhoR; ABC-type nitrate/sulfonate/bicarbonate transport system, permease component	*Candidatus Accumulibacter, Oblitimonas, Pseudoxanthomonas, Polyangium brachysporum*
Metal resistance/transport genes		
Iron	ABC-type Fe^{3+}-hydroxamate transport system, periplasmic component; Outer membrane receptor for ferrienterochelin and colicins, FepA; siderophore synthetase component; ferrichrome/ferrioxamine B periplasmic transporter; ABC.FEV.S, iron complex transport system substrate-binding protein; ofuC, fbpC, Fe^{3+} transport system ATP-binding protein; TC.FEV.OM, iron complex outer membrane receptor protein; bacterioferritin	*Stenotrophomonas, Pseudomonas, Gluconacetobacter, Zhongshania, Phenylobacterium*
Cadmium, lead, zinc, mercury and manganese	Zinc/cadmium/mercury/lead transporting ATPase; Cd^{2+}/Zn^{2+}-exporting ATPase, zntA; Mn^{2+} and Fe^{2+} transporters of the NRAMP family; manganese transport protein, MntH	*Candidatus Accumulibacter, Pseudomonas geniculata*
Copper and silver	Putative silver efflux pump; CueR, MerR family transcriptional regulator, copper efflux regulator; Cu(I)/Ag(I) efflux system membrane protein CusA/SilA	*Stenotrophomonas, Immundisolibacter, Dyella*

Table 5 List of genes coding for enzymes identified in 3S polluted system involved in hydrocarbon degradation

Enzyme	Enzyme function	Bit score	*e* value
Rieske non-heme iron oxygenase (RO)	Involved in regio- and stereoselective transformation of a wide array of aromatic hydrocarbons	86.12	$6.87e^{-24}$
Rieske non-heme iron oxygenase (RO), α-subunit	The catalytic domain of RO, aromatic ring-hydroxylating dioxygenases	49.89	$1.67e^{-09}$
Vanillate *O*-demethylase oxygenase subunit	Catalyzes the reductive conversion of vanillate into protocatechuate and formaldehyde	43.12	$7.72e^{-07}$
Dicamba *O*-demethylase oxygenase	Catalyzes the conversion of dicamba (2-methoxy-3,6-dichlorobenzoic acid) to DCSA (3,6-dichlorosalicylic acid)	43.12	$7.72e^{-07}$
Phenylpropionate dioxygenase, large terminal subunit	Catalyse the Insertion of both atoms of molecular oxygen into positions 2 and 3 of the phenyl ring of phenylpropionate, yielding cis-3-(3-carboxyethyl)-3,5-cyclohexadiene-1,2-diol	44.41	$8.48e^{-07}$
Rieske non-heme iron oxygenase (RO), ferredoxin component of biphenyl dioxygenase (BPDO) and carbazole 1,9a-dioxygenase (CARDO)	BPDO degrades biphenyls and polychlorinated biphenyls. CARDO catalyzes angular dioxygenation of carbazole at the C1 and C9a positions	41.32	$2.47e^{-06}$
2-keto-4-pentenoate hydratase/2-oxohepta-3-ene-1,7-dioic acid hydratase (catechol pathway)	Catechol pathway	51.59	$1.89e^{-09}$
4-hydroxyphenylacetate degradation bifunctional isomerase/decarboxylase, C-terminal subunit	Decarboxylate OPET to HHDD; isomerize HHDD to OHED (4-hydroxyphenylacetate degradation)	45.57	$1.98e^{-07}$
2,3-dihydro-2,3-dihydroxybenzoate dehydrogenase	Catalyzes the NAD+-dependent oxidation of 2,3-dihydro-2,3-dihydroxybenzoate to produce an aromatic compound 2,3-didihydroxybenzoic acid	60.76	$1.88e^{-12}$
2-hydroxycyclohexanecarboxyl-CoA dehydrogenase	Catalyze the anaerobic degradation of benzoyl-CoA to 3-hydroxypimeloyl-CoA	57.24	$3.92e^{-11}$
1,6-dihydroxycyclohexa-2,4-diene-1-carboxylate dehydrogenase (DHB-DH)	Catalyzes the NAD-dependent conversion of 1,2-dihydroxycyclohexa-3,4-diene carboxylate to a catechol	56.77	$6.19e^{-11}$
cis-biphenyl-2,3-dihydrodiol-2,3-dehydrogenase (BphB)	Biphenyl/polychlorinated biphenyl degradation pathway	40.03	$6.01e^{-05}$
Cyclohexanol reductase	Catalyse the reversible oxidoreduction of hydroxycyclohexanone derivatives	55.99	$1.23e^{-10}$
Cyclohexanecarboxyl-CoA dehydrogenase	Funnel the alicyclic acid cyclohexane carboxylate into the anaerobic benzoate degradation pathway	45.68	$2.44e^{-07}$
Dibenzothiophene (DBT) desulfurization enzyme C; DszC	Converts DBT to DBT-sulfoxide, which is then converted to DBT-sulfone	33.07	$6.14e^{-03}$
3-Oxoadipyl-CoA thiolase	Participates in benzoate degradation via hydroxylation	105.64	$6.67e^{-28}$
Acetyl-CoA acetyltransferases	Fatty acid degradation, benzoate degradation, ethylbenzene degradation	153.92	$2.60e^{-46}$
C-terminal substrate binding domain of LysR-type transcriptional regulators involved in the catabolism of aromatic compounds	Involved in degradation of aromatic compounds	80.63	$1.43e^{-20}$
C-terminal substrate binding domain of LysR-type transcription regulators, BenM, CatM, and CatR	Participate in benzoate degradation	48.76	$1.71e^{-08}$
C-terminal substrate binding domain of LysR-type transcriptional regulators that involved in the catabolism of nitroaromatic/naphthalene compounds	Involved in the degradation of dinitrotoluene and similar compounds	43.74	$1.06e^{-06}$
C-terminal substrate binding domain of LysR-type transcriptional regulators CbnR, ClcR and TfdR	Participate in the regulation of chlorocatechol catabolism	39.19	$3.95e^{-05}$
pca operon transcription factor PcaQ	Catabolism of protocatechuate	35.46	$1.09e^{-03}$

Table 6 List of gene coding for enzymes detected in AB4 polluted system involved in hydrocarbon degradation

Enzyme	Enzyme function	Bit score	*e* value
Rieske non-heme iron oxygenase (RO)	Involved in regio- and stereoselective transformation of a wide array of aromatic hydrocarbons	86.12	$1.90e^{-23}$
Rieske non-heme iron oxygenase (RO), α-subunit	The catalytic domain of RO, aromatic ring-hydroxylating dioxygenases	50.66	$2.48e^{-09}$
Vanillate *O*-demethylase oxygenase subunit	Catalyzes the reductive conversion of vanillate into protocatechuate and formaldehyde	43.51	$1.38e^{-06}$
Dicamba *O*-demethylase oxygenase	Catalyses the conversion of dicamba (2-methoxy-3,6-dichlorobenzoic acid) to DCSA (3,6-dichlorosalicylic acid)	43.51	$1.38e^{-06}$
Rieske non-heme iron oxygenase (RO), ferredoxin component of biphenyl dioxygenase (BPDO) and carbazole 1,9a-dioxygenase (CARDO)	BPDO degrades biphenyls and polychlorinated biphenyls. CARDO catalyses angular dioxygenation of carbazole at the C1 and C9a positions	41.70	$3.93e^{-06}$
Anthranilate 1,2-dioxygenase (AntDO)	AntDO converts anthranilate to catechol	35.52	$2.06e^{-03}$
Phthalate 4,5-dioxygenase (PhDO) oxygenase α-subunit	Catalyzes the dihydroxylation of phthalate to form the 4,5-dihydro-cis-dihydrodiol of phthalate (DHD)	45.57	$1.98e^{-07}$
2-Oxoquinoline 8-monooxygenase (OMO)	Participate in quinoline degradation via the NADH-dependent oxidation of 2-oxoquinoline to 8-hydroxy-2-oxoquinoline	33.93	$2.60e^{-03}$
Phenylpropionate dioxygenase, large terminal subunit	Catalyse the Insertion of both atoms of molecular oxygen into positions 2 and 3 of the phenyl ring of phenylpropionate, yielding cis-3-(3-carboxyethyl)-3,5-cyclohexadiene-1,2-diol	46.33	$5.21e^{-07}$
Aldehyde dehydrogenase	Participate in alkane metabolism, Fatty acid degradation, chloroalkane and chloroalkene degradation	77.65	$1.57e^{-18}$
$NAD(P)^+$-dependent benzaldehyde dehydrogenase II, p-hydroxybenzaldehyde dehydrogenase and related proteins	benzaldehyde dehydrogenase II catalyses the oxidation of benzyl alcohol to benzoate; p-hydroxybenzaldehyde dehydrogenase catalyses the oxidation of p-hydroxybenzaldehyde to p-hydroxybenzoic acid	60.24	$2.01e^{-12}$
Phenylacetaldehyde dehydrogenase (PADH); NahF salicylaldehyde dehydrogenase	StyD PADH involved in styrene catabolism; salicylaldehyde dehydrogenase catalyses the conversion of salicylaldehyde to salicylate	55.91	$7.98e^{-11}$
NAD^+-dependent chloroacetaldehyde dehydrogenases (AldA and AldB)	Participate in the degradation of 1,2-dichloroethane	51.58	$2.48e^{-09}$
4-Hydroxymuconic semialdehyde dehydrogenase	Involved in 4-hydroxyacetophenone degradation	55.99	$1.47e^{-11}$
Vanillin dehydrogenase	Oxidation of vanillin to vanillinic acid; involved in benzaldehyde, protocatechualdehyde m-anisaldehyde, and p-hydroxybenzaldehyde degradation	54.26	$2.64e^{-10}$
p-Hydroxybenzaldehyde dehydrogenase	Catalyses oxidation of p-hydroxybenzaldehyde to p-hydroxybenzoic acid	49.22	$1.68e^{-08}$
5-Carboxymethyl-2-hydroxymuconate semialdehyde dehydrogenase	Transform 5-carboxymethyl-2-hydroxymuconate semialdehyde (CHMS) to 5-carboxymethyl-2-hydroxymuconate (CHM) (4-hydroxyphenylacetate degradation)	49.03	$1.93e^{-08}$
Salicylaldehyde dehydrogenase	Involved in the upper naphthalene catabolic pathway	48.73	$2.59e^{-08}$
2-Hydroxymuconic semialdehyde dehydrogenase	Catalyzes the second step in *meta*-cleavage pathway for catechol degradation	48.57	$2.66e^{-08}$
2-Carboxybenzaldehyde dehydrogenase, PhdK	Involved in phenanthrene degradation	45.06	$4.83e^{-07}$
Cyclohexanecarboxyl-CoA dehydrogenase	Funnel the alicyclic acid, cyclohexane carboxylate into the anaerobic benzoate degradation pathway	38.36	$1.53e^{-04}$
Anaerobic benzoate catabolism transcriptional regulator	Involved in anaerobic catabolism of benzoate	43.79	$3.83e^{-06}$

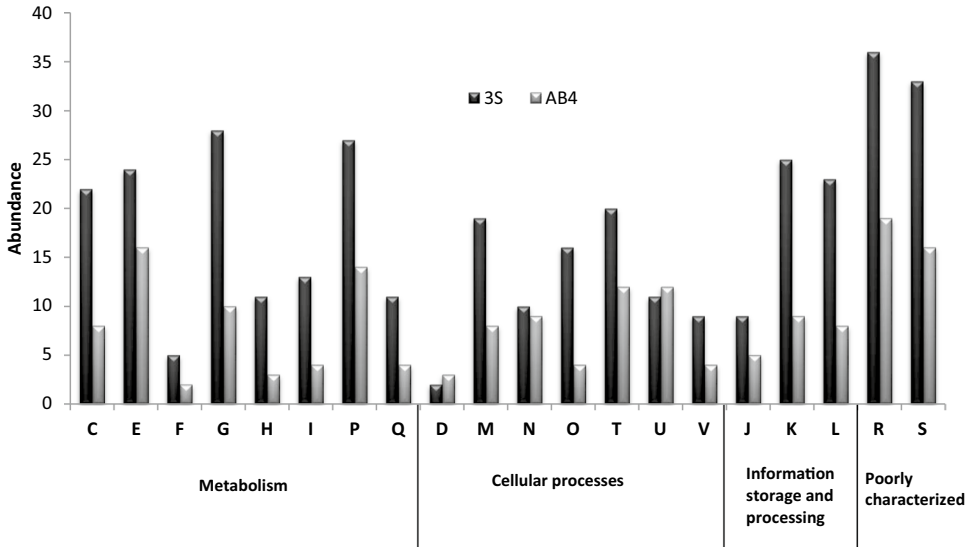

Fig. 6 Functional characterization of metagenomic reads of 3S and AB4 microcosms according to the Cluster of Orthologous Groups of protein (COGs). The categories for COG are abbreviated as follows: C: energy production and conversion; E: amino acid transport and metabolism; F: nucleotide transport and metabolism; G: carbohydrate transport and metabolism; H: coenzyme transport and metabolism; I: lipid transport and metabolism; P: inorganic ion transport and metabolism; Q: secondary metabolites biosynthesis, transport and metabolism; D: cell cycle control, cell division, chromosome partitioning; M: cell wall/membrane/envelope biogenesis; N: cell motility; O: post-translational modification, protein turnover, chaperones; T: signal transduction mechanism; U: intracellular trafficking, secretion and vesicular transport; V: defense mechanisms; J: translation, ribosomal structure and biogenesis; K: transcription; L: replication, recombination and repair; R: general function prediction only; S: function unknown

phenomenon to complexation of hydrocarbons with essential inorganic nutrients such as nitrates, phosphates, and sulfates needed for microbial growth and metabolic activities (Andrew and Jackson 1996; Adebusoye et al. 2010). This led to destruction of these essential nutrients and render them inaccessible to microbial uptake, thus impeding pollutant removal.

In this study, the microbial community of the two microcosms, 3S and AB4 displayed extensive hydrocarbon degradation potentials as reflected in the aliphatic and aromatic degradation rates in 3S (aliphatic 61.27%; aromatic 66.58%) and AB4 (aliphatic 95.95%; aromatic 94.60%) microcosms. This is not surprising as the sampling site has been inundated with hydrocarbon inputs for several years thus allowing intrinsic adaptation of the microbial community to the pollutants and the evolution of diverse degradative genes via enzyme induction, mutation, DNA rearrangement and horizontal gene transfer (Top and Springael 2003; Maier 2009). The higher degradation rate observed in CSL-amended AB4 could be attributed to the presence of essential nutrient sources and growth factors in CSL, which stimulate and enhance the degradation ability of the microbial community.

Observation of degradation patterns of the hydrocarbon constituents in 3S and AB4 systems indicate significant differences. First, most of the short and long straight chain aliphatics were completely degraded in AB4 system at the end of 42 days in contrast to 3S system, which has only ethane and heneicosane completely degraded during the same period. Similarly, most of the aromatic constituents in AB4 system were either completely degraded or degraded to $< 10\%$ of their initial concentrations in contrast to 3S system, which exhibited lower degradation rates. The observed differences could be attributed to the CSL amendment of AB4 system, which provided the elusive inorganic macronutrients and growth factors required by the microbial community for sugar phosphorylation, synthesis of amino acids, nucleic acids, nucleotides, and other cellular processes (Andrew and Jackson 1996). The presence of these nutrients stimulates the growth and proliferation of the microbial cells and enhance the rate of degradation of the pollutants. Furthermore, the broad spectrum of aliphatic and aromatic substrates degradable by 3S and AB4 microbial communities may not be unconnected to the huge catabolic diversity present in the communities and the relaxed substrate specificity of some of the catabolic pathways (Perez-Pantoja et al. 2008).

Structural analyses of the two polluted systems, 3S and AB4 showed the predominance of *Actinobacteria* (31.46%) and *Proteobacteria* (38.95%). This is expected as the two phyla harbours members that are promising candidates for depuration of hydrocarbon-polluted soils. *Actinobacteria* colonizes soil particles through their filamentous growth, produces spores that are impervious to desiccation and other harsh environmental conditions, and secretes extracellular enzymes that catalyse a wide range of complex organic

compounds and pollutants (Ensign 1992; Larkin et al. 2005). Furthermore, the genetic plasticity, metabolic versatility and production of extracellular and cellular biosurfactants by members of *Actinobacteria*, which enhances the uptake and biodegradation of hydrophobic pollutants (Singer and Finnerty 1990; Morikawa et al. 1993; Neu 1996; Mutnuri et al. 2005; Kanaly and Harayama 2010) may also account for the predominance of this phylum in 3S polluted system.

While the phylum *Proteobacteria* account for 19.52% of the sequence reads in 3S, it accounted for 38.95% in AB4 polluted system. Though members of *Proteobacteria* due to their catabolic versatility, genetic plasticity and metabolic diversity have broad substrate specificities for several classes of hydrocarbons (Nojiri et al. 1999; Habe et al. 2002; Salam et al. 2014), their enrichment in AB4 system may not be unconnected to the CSL amendment. The α, β, and γ classes of *Proteobacteria* are regarded as copiotrophs, thus, the addition of CSL rich in utilizable carbon and other nutrients could be responsible for the surge in population of the phylum *Proteobacteria* in AB4 system (Fierer et al. 2007; Eilers et al. 2010; Goldfarb et al. 2011).

The predominance of the genera *Verticillium* and *Laceyella* in 3S and AB4 systems is quite novel and interesting. The phylum *Ascomycota* to which *Verticillium* is a member comprises of representatives that are well adapted to hydrocarbon-contaminated matrices. They have been recovered from hydrocarbon-contaminated aquatic and terrestrial environments (Atlas 1981; Simister et al. 2015; Kachienga et al. 2018), implicated in PAHs transformation (Aranda 2016; Godoy et al. 2016) and the degradation of quaternary ammonium compounds (QACs) and long chain alkylbenzenes (Fedorak and Westlake 1986; Zabielska-Matejuk and Czaczyk 2006). Other genera with higher representations in 3S such as *Microbacterium, Dethiobacter, Brevibacterium* and *Pseudomonas* have been recovered severally from diverse hydrocarbon-polluted environments (Schippers et al. 2005; Manickam et al. 2006; Salam et al. 2014, 2017; Muangchinda et al. 2015; Graziano et al. 2016).

Members of the genus *Laceyella* belonging to the phylum *Firmicutes* are Gram-positive, aerobic, endospore-forming, chemoorganotrophic thermophilic filamentous bacteria that have been isolated from diverse environments such as hot spring (Chen et al. 2012), soil from a volcano (Zhang et al. 2010a, b) and subtropical environment (Carrillo et al. 2009). They are efficient producers of carbohydrate-degrading enzymes such as α-amylase, xylanase, poly(L-lactide)-degrading enzymes, and raw starch degrading enzymes among others (Singh et al. 2012; Hanphakphoom et al. 2014; Lomthong et al. 2015; El-Sayed et al. 2017). Their preponderance in AB4 system could be attributed to endospore formation, which allow them to adapt and survive the harsh environmental conditions in the polluted soil; and production of carbohydrate active enzymes, which allow them to metabolize the carbohydrates in the CSL as carbon source. The detection of the enzymes isoamylase (EC 3.2.1.68) and 1,4-alpha-glucan branching enzyme (EC 2.4.1.18) in AB4 polluted system give credence to this assertion. While members of the phylum *Firmicutes* have been recovered from several hydrocarbon-polluted niches, globally, only one report mentions the recovery of *Laceyella* species from soils historically contaminated by heavy metals and hydrocarbons (Vivas et al. 2008). Other genera with significant representations in AB4 systems such as *Methylosinus, Pedobacter* and *Terrimonas* have been implicated in the degradation of short- and long-chain aliphatic hydrocarbons, halogenated hydrocarbons, and polycyclic aromatic hydrocarbons (Oldenhuis et al. 1989; DeFlaun et al. 1992; Lee et al. 2006; Zhang et al. 2011; Margesin and Zhang 2013; Singleton et al. 2016).

Functional analyses of the two polluted systems 3S and AB4 revealed interesting features. The SEED subsystem showed similarities of the two systems in most of the features such as metabolism of aromatic compounds, membrane transport, clustering-based subsystems, protein metabolism among others (Fig. 6). The detection of potassium metabolism in AB4 (which is not detected in 3S) and the upscale of nitrogen metabolism in AB4 could be attributed to amendment of AB4 system with CSL. Among the many pollutants synonymous with hydrocarbon-polluted soils is the presence of heavy metals (Salam et al. 2014, 2017; Salam 2016). As shown in Tables 3 and 4, the presence of various heavy metals in the two systems and the detection of several efflux systems and resistance genes used by the microbial communities to circumvent the heavy metals stress and toxicity is an attestation to the adaptation and resistance of some members of the microbial community to the heavy metals stress. Though microorganisms have devised various resistance mechanisms such as reduction of a metal to a less toxic species, formation and sequestration of heavy metals in complexes, and direct efflux of a metal out of the cell; the role of mobile genetic elements and horizontal gene transfer (HGT) in the distribution of these resistance mechanisms in the microbial community cannot be overemphasized (Nucifora et al. 1989; Lin and Olson 1995; Nies and Silver 1995; Outten et al. 2000; Spain and Alm 2003; Villadangos et al. 2012). This assertion is further buttressed by the detection of diverse genera of the microbial communities cutting across different phyla harbouring heavy metals resistance genes and efflux systems (Tables 3, 4), thus suggesting the involvement of HGT facilitated by heavy metal resistance genes borne on mobile genetic elements (Endo et al. 2002; Nemergut et al. 2004).

The Rieske non-heme iron oxygenases (ROs), a multicomponent enzyme complex consisting of a terminal oxygenase component and different electron transport proteins are family of enzymes that mediate the aerobic activation and thus

degradation of aromatic hydrocarbons such as benzoate, benzene, toluene, phthalate, naphthalene or biphenyl (Gibson and Parales 2000; Pérez-Pantoja et al. 2010). These enzymes catalyse the incorporation of two oxygen atoms into the aromatic ring to form arene-cis-dihydrodiols, which is followed by a dehydrogenation usually catalysed by cis-dihydrodiol dehydrogenases to give (substituted) catechols. Enzymes belonging to this family catalyzed diverse dioxygenations of aromatics, polyaromatics, and heteroaromatic hydrocarbons resulting in regio- and stereoselective transformations (Nojiri et al. 1999, 2001; Perez-Pentoja et al. 2012). As shown in Tables 5 and 6, the detection of various enzymes of the ROs family in both polluted systems underscore the importance of ROs in aerobic degradation of aromatic hydrocarbons. This perhaps explain the extensive degradation of aromatic fractions of the hydrocarbons in the polluted systems, though more pronounced in AB4 system due to CSL amendment.

More interesting is the detection of enzymes of the aldehyde dehydrogenase (ALDH) superfamily in AB4 system that are not detected in 3S system. ALDH is a divergently related group of enzymes that oxidize a broad range of aliphatic and aromatic aldehydes to their corresponding carboxylic acids (Vasiliou et al. 2000; Sophos and Vasiliou 2003). ALDH also played prominent role in alkane oxidation and help in detoxification of the toxic aldehydes produced by several cellular metabolic pathways (Rojo 2009; Talfournier et al. 2011; Esser et al. 2013). Aside from CSL amendment of AB4 system that played significant role in enhanced degradation, the detection of diverse enzyme systems with relaxed and broad substrate specificities may have also contributed immensely to the enhanced degradation observed in the polluted system.

In any polluted environment, plethora of pollutants are always present requiring the deployment of diverse catabolic pathways for their degradation. It is therefore not surprising that the microbial community in the two polluted systems utilizes various catabolic enzymes and genes belonging to various families such as Rieske non-heme dioxygenases, FAA hydrolases, short-chain dehydrogenases/reductases, acyltransferases, among others for the degradation of pollutants (Tables 5, 6). This shows extensive realignments and recruitments of degradative genes since the sequence reads from the polluted systems contain aggregation of genes belonging to different pathways previously described for aerobic and anaerobic degradation of different aromatic and aliphatic compounds.

Conclusions

This study has established the importance of CSL as a biostimulant used to enhance degradation of hydrocarbon pollutants. It also showcased the degradation competencies of diverse members of the microbial community hitherto not reported as important players in remediation of hydrocarbon-polluted soils. In addition, this study also reveals the indisputable fact that consortium of microorganisms and their catabolic enzymes systems acquired via promiscuous recruitments and realignments is pivotal for remediation of environments polluted with diverse hydrocarbon pollutants.

References

Adebusoye SA, Ilori MO, Obayori OS, Oyetibo GO, Akindele KA, Amund OO (2010) Efficiency of cassava steep liquor for bioremediation of diesel oil-contaminated tropical agricultural soil. Environmentalist 30:23–24

Alexander M (1999) Biodegradation and bioremediation, 2nd edn. Academic Press, San Diego

Amadi A, Bari YU (1992) Use of poultry manure for amendment of oil polluted soils in relation to the growth of maize (*Zea mays*). Environ Int 18:521–552

Andrew RWJ, Jackson JM (1996) Pollution and waste management. In: The natural environment and human impact. Longman Publishers, Singapore, pp 281–297

Aranda E (2016) Promising approaches towards biotransformation of polycyclic aromatic hydrocarbons with Ascomycota fungi. Curr Opin Biotechnol 38:1–8

Atlas RM (1981) Microbial degradation of petroleum: an environmental perspective. Microbiol Rev 45:180–209

Bashir Y, Singh SP, Konwar BK (2014) Metagenomics: an application-based perspective. Chinese J Biol https://doi.org/10.1155/2014/146030

Bossert I, Bartha R (1984) The fate of fuel spills in soil ecosystems. In: Atlas RM (ed) Petroleum microbiology. Macmillan, New York, pp 435–473 In

Bundy JG, Paton GI, Campbell CD (2002) Microbial communities in different soils do not converge after diesel contamination. J Appl Microbiol 92:276–288

Carrillo L, Ahrendts MRB, Maldonado MJ (2009) Alkalithermophilic actinomycetes in a subtropical area of Jujuy, Argentina. Revista Argentina de Microbiología 41:112–116

Chen J-J, Lin L-B, Zhang L-L, Zhang J, Tang S-K, Wei Y-L, Li W-J (2012) *Laceyella sediminis* sp. nov., a thermophilic bacterium isolated from a hot spring. Int J Syst Evol Microbiol 62:38–42

Chiani M, Akbarzadeh A, Farhangi A, Mehrabi MR (2010) Production of desferrioxamine B (Desfaral) using corn steep liquor in *Streptomyces pilosus*. Pak J Biol Sci 13:1151–1155

Cox MP, Peterson DA, Biggs PJ (2010) SolexaQA: at a glance quality assessment of illumine second-generation sequencing data. BMC Bioinform 11:485

DeFlaun MF, Ensley BD, Steffan RJ (1992) Biological oxidation of hydrochlorofluorocarbons (HCFCs) by a methanotrophic bacterium. Biotechnol 10:1576–1578

Eilers KG, Lauber CL, Knight R, Fierer N (2010) Shifts in bacterial community structure associated with inputs of low molecular weight carbon compounds to soil. Soil Biol Biochem 42:896–903

El-Sayed AK, Abou-Dobara MI, El-Fallal A, Omar NF (2017) Gene sequence, modeling, and enzymatic characterization of α-amylase AmyLa from the thermophile *Laceyella* sp. DS3. Starch 69(5–6):1–9

Endo G, Narita M, Huang CC, Silver S (2002) Microbial heavy metal resistance transposons and plasmids: potential use for environmental biotechnology. J Environ Biotechnol 2:71–82

Ensign JC (1992) Introduction to the actinomycetes. In: Ballows A, Truper HG, Dworkin M, Harder W, Schleifer KH (eds) the Prokaryotes. a handbook on the biology of bacteria, ecophysiology, isolation, identification, application. Springer, New York, pp 811–815

Esser D, Kouril T, Talfournier F et al (2013) Unravelling the function of paralogs of the aldehyde dehydrogenase super family from *Sulfolobus solfataricus*. Extremophiles 12:75–88

Fedorak PM, Westlake DWS (1986) Fungal metabolism of n-alkylbenzenes. Appl Environ Microbiol 51(2):435–437

Fierer N, Bradford MA, Jackson RB (2007) Towards an ecological classification of soil bacteria. Ecology 88:1354–1364

Filipovic SS, Ristc MD, Sakac MB (2002) Technology of corn steep liquor application in animal mashes and their quality. Roum Biotechnol Lett 7:705–710

Fox JL (2011) Natural-born eaters. Nat Biotechnol 29:103–106

Gibson DT, Parales RE (2000) Aromatic hydrocarbon dioxygenases in environmental biotechnology. Curr Opin Biotechnol 11:236–243

Godoy P, Reina R, Calderón A, Wittich R-M, García-Romera I, Aranda E (2016) Exploring the potential of fungi isolated from PAH-polluted soil as a source of xenobiotics-degrading fungi. Environ Sci Polut Res. https://doi.org/10.1007/s11356-016-7257-1

Goldfarb KC, Karaoz U, Hanson CA et al (2011) Differential growth responses of soil bacterial taxa to carbon substrates of varying chemical recalcitrance. Front Microbiol 2:94

Graziano M, Rizzo C, Michaud L, Porporato EMD, De Domenico E, Spano N, Lo Giudice A (2016) Biosurfactant production by hydrocarbon degrading *Brevibacterium* and *Vibrio* isolates from the sea pen *Pteroeides spinosum* (Ellis, 1764). J Basic Microbiol 56(9):963–974

Habe H, Chung JS, Lee JH, Kasuga K, Yoshida T, Nojiri H, Omori T (2001) Degradation of chlorinated dibenzofurans and dibenzo-p-dioxins by two types of bacteria having angular dioxygenases with different features. Appl Environ Microbiol 67:3610–3617

Habe H, Ashikawa Y, Saiki Y, Yoshida T, Nojiri H, Omori T (2002) *Sphingomonas* sp. strain KA1, carrying a carbazole dioxygenase gene homologue, degrades chlorinated dibenzo-p-dioxins in soil. FEMS Microbiol Lett 211:43–49

Handelsman J (2004) Metagenomics: application of genomics to uncultured microorganisms. Microbiol Mol Biol Rev 68:669–678

Hanphakphoom S, Maneewong N, Sukkhum S, Tokuyama S, Kitpreechavanich V (2014) Characterization of poly(L-lactide)-degrading enzyme produced by thermophilic filamentous bacteria *Laceyella sacchari* LP175. J Gen Appl Microbiol 60:13–22

Kachienga L, Jitendra K, Momba M (2018) Metagenomic profiling for assessing microbial diversity and microbial adaptation to degradation of hydrocarbons in two South African petroleum contaminated water aquifers. Sci Rep 8:7564

Kanaly RA, Harayama S (2010) Advances in the field of high molecular-weight polycyclic aromatic hydrocarbon biodegradation by bacteria. Microbiol Biotechnol 3(2):132–164

Kanehisa M, Sato Y, Morishima K (2016) BlastKOALA and GhostKOALA: KEGG tools for functional characterization of genome and metagenome sequences. J Mol Biol 428(4):726–731

Keegan KP, Glass EM, Meyer F (2016) MG-RAST, a metagenomics service for analysis of microbial community structure and function. Methods Mol Biol 1399:207–233

Langmead B, Salzberg SL (2012) Fast gapped-read alignment with Bowtie-2. Nat Methods 9(4):357–359

Larkin MJ, Kulakov LA, Allen CC (2005) Biodegradation and *Rhodococcus*-masters of catabolic versatility. Curr Opin Biotechnol 16:282–290

Lawford HG, Rousseau JD (1997) Corn steep liquor as a cost-effective nutrition adjunct in high performance *Zymomonas* ethanol fermentation. Appl Biochem Biotechnol 63–65:287–304

Liggert RW, Koffler H (1948) Corn steep liquor in microbiology. Bacteriol Rev 12(4):297–311

Lin C, Olson BH (1995) Occurrence of cop-like resistance genes among bacteria isolated from a water distribution system. Can J Microbiol 41:642–646

Lomthong T, Chotineeranat S, Kitpreechavanich V (2015) Production and characterization of raw starch degrading enzyme from a newly isolated thermophilic filamentous bacterium, *Laceyella sacchari* LP175. Starch 67(3–4):255–266

Maddipati P, Atiyeh HK, Bellmer DN, Huhnke RL (2011) Ethanol production from Syngas by *Clostridium* strain P11 using corn steep liquor as a nutrient replacement to yeast extract. Biores Technol 102:6494–6501

Maier RM (2009) Microorganisms and organic pollutants. In: Maier RM, Pepper IL, Gerba CP (eds) Environmental microbiology, second edn. Academic Press, London, pp 387–420

Maier RM, Pepper IL, Gerba CP (2000) Environmental microbiology. Academic Press, London

Manickam N, Mau M, Schlo¨mann M (2006) Characterization of the novel HCH-degrading *Microbacterium* sp. ITRC1. Appl Microbiol Biotechnol 69:580–588

Marchler-Bauer A, Derbyshire MK, Gonzales NR et al (2015) CDD: NCBI's conserved domain database. Nucleic Acids Res 43(D):222–226

Margesin R, Zhang D-C (2013) Pedobacter *ruber* sp. nov., a psychrophilic bacterium isolated from soil. Int J Syst Evol Microbiol 63:339–344

Morikawa M, Daido H, Takao T, Murata S, Shimonishi Y, Imanaka T (1993) A new lipopeptide biosurfactant produced by *Arthrobacter* sp. strain MIS38. J Bacteriol 175:6459–6466

Muangchinda C, Chavanich S, Viyakarn V, Watanabe K, Imura S, Vangnai AS, Pinyakong O (2015) Abundance and diversity of functional genes involved in the degradation of aromatic hydrocarbons in Antarctic soils and sediments around Syowa Station. Environ Sci Pollut Res 22:4725–4735

Mutnuri S, Vasudevan N, Kaestner M (2005) Degradation of anthracene and pyrene supplied by microcrystals and nonaqueous-phase liquids. Appl Microbiol Biotechnol 67:569–576

Nemergut DR, Martin AP, Schmidt SK (2004) Intergon diversity in heavy-metal-contaminated mine tailings and inferences about integron evolution. Appl Environ Microbiol 70:1160–1168

Neu TR (1996) Significance of bacterial surface-active compounds in interaction of bacteria with interfaces. Microbiol Rev 60:151–166

Nies DH, Silver S (1995) Ion efflux systems involved in bacterial metal resistances. J Ind Microbiol 14:186–199

Nojiri H, Nam J-W, Kosaka M et al (1999) Diverse oxygenations catalyzed by carbazole 1,9a-dioxygenase from *Pseudomonas* sp. strain CA10. J Bacterio 181(10):3105–3113

Nojiri H, Habe H, Omori T (2001) Bacterial degradation of aromatic compounds via angular dioxygenations. J Gen Appl Microbiol 47:279–305

Nucifora G, Chu L, Misra TK, Silver S (1989) Cadmium resistance from Staphylococcus aureus plasmid p1258 cadA gene results from cadmium-efflux ATPase. Proc Natl Acad Sci USA 86:3544–3548

Obayori OS, Ilori MO, Adebusoye SA, Amund OO, Oyetibo GO (2008) Microbial population changes in tropical agricultural soil experimentally contaminated with crude petroleum. Afr J Biotechnol 7:4512–4520

Obayori OS, Ilori MO, Adebusoye SA, Oyetibo GO, Omotayo AE, Amund OO (2010) Effects of corn steep liquor on growth rate and pyrene degradation by *Pseudomonas* strains. Current Microbiol 60:407–411

Obayori OS, Salam LB, Anifowoshe WT, Odunewu ZM, Amosu OE, Ofulue BE (2015) Enhanced Degradation of Petroleum

Hydrocarbons in Corn-Steep-Liquor-Treated Soil Microcosm. Soil Sediment Contam 24(7):731–743
Okoh AI (2006) Biodegradation alternative in the clean-up of petroleum hydrocarbon pollutants. Biotechnol Mol Biol Rev 1:38–50
Okolo JC, Amadi EN, Odu CTI (2005) Effect of soil treatments containing poultry manure on crude oil degradation in a sandy loam soil. Appl Ecol Environ Res 3:47–55
Oldenhuis R, Vink RL, Janssen DB, Witholt B (1989) Degradation of chlorinated aliphatic hydrocarbons by *Methylosinus trichosporium* OB3b expressing soluble methane monooxygenase. Appl Environ Microbiol 55(11):2819–2826
Oulas A, Pavloudi G, Polymanakou P, Pavlopoulus GA, Papanikolaou N, Kotoulas G, Arvanitidis C, Iliopoulus I (2015) Metagenomics: tools and insights for analyzing next-generation sequencing data derived from biodiversity studies. Bioinform Biol Insights 9:75–88
Outten FW, Outten CE, O'Halloran T (2000) Metalloregulatory systems at the interface between bacterial metal homeostasis and resistance. In: Storz G, Hengge-Aronis R (eds) Bacterial stress responses. ASM Press, Washington D.C, pp 145–157
Parks DH, Tyson GW, Hugenhiltz P, Beiko RG (2014) STAMP: statistical analysis of taxonomic and functional profiles. Bioinformatics 30(21):3123–3124
Perez-Pantoja D, De la Iglesia R, Pieper DH, Gonzalez B (2008) Metabolic reconstruction of aromatic compounds degradation from the genome of the amazing pollutant-degrading bacterium *Cupriavidus necator* JMP134. FEMS Microbiol Rev 32:736–794
Pérez-Pantoja D, González B, Pieper DH (2010) Aerobic degradation of aromatic hydrocarbons. In: Timmis KN (ed) Handbook of hydrocarbon and lipid microbiology. Springer, Berlin, pp 799–837
Perez-Pentoja D, Donoso R, Agullo L, Cordova M, Seeger M, Pieper DH, Gonzalez B (2012) Genomic analysis of the potential for aromatic compounds biodegradation in *Burkholderiales*. Environ Microbiol 14(5):1091–1117
Philp JC, Bamforth SM, Singleton I, Atlas RM (2005) Environmental pollution and restoration: a role for bioremediation. In: Atlas RM, Philp J (eds) Applied microbial solutions for real-world environmental clean-up. ASM, Washington, DC, pp 1–48
Pritchard RH, Mueller JG, Rogers JC, Kremer FV, Glaser JA (1992) Oil spill bioremediations: experiences, lesson, and results from the Exxon Valdez oil spill in Alaska. Biodegradation 3:315–335
Rho M, Tang H, Ye Y (2010) FragGeneScan: predicting genes in short and error-prone reads. Nucleic Acid Res 38:20–191
Rojo F (2009) Degradation of alkanes by bacteria. Environ Microbiol 11(10):2477–2490
Saha BC, Racine FM (2010) Effect of pH and corn steep liquor variability on mannitol production by *Lactobacillus intermidius* NRRL B-3693. Appl Microbiol Biotechnol 87:553–556
Salam LB (2016) Metabolism of waste engine oil by *Pseudomonas* species. 3 Biotech 6(1):1–10
Salam LB, Ilori MO, Amund OO et al (2014) Carbazole angular dioxygenation and mineralization by bacteria isolated from hydrocarbon-contaminated tropical African soil. Environ Sci Pollut Res 21:9311–9324
Salam LB, Ilori MO, Amund OO (2015) Carbazole degradation in the soil microcosm by tropical bacterial strains. Brazilian J Microbiol 46(4):1037–1044
Salam LB, Obayori OS, Nwaokorie FO, Suleiman A, Mustapha R (2017) Metagenomic insights into effects of spent engine oil perturbation on the microbial community composition and function in a tropical agricultural soil. Environ Sci Pollut Res 24:7139–7159
Salam LB, Ilori MO, Amund OO, LiiMien Y, Nojiri H (2018) Characterization of bacterial community structure in a hydrocarbon-contaminated tropical African soil. Environ Technol 39(7):939–951
Schippers A, Bosecker K, Spro¨er C, Schumann P (2005) *Microbacterium oleivorans* sp. nov. and *Microbacterium hydrocarbonoxydans* sp. nov., novel crude-oil-degrading Gram-positive bacteria. Int J Syst Evol Microbiol 55:655–660
Schloss PD, Westcott SL, Ryabin T et al (2009) Introducing mother: open-source, platform-independent, community-supported software for describing and comparing microbial communities. Appl Environ Microbiol 75(23):7537–7541
Simister R, Poutasse CM, Thurston A, Reeve J, Baker MC, White HK (2015) Degradation of oil by fungi isolated from Gulf of Mexico beaches. Mar Pollut Bull 100(1):327–333
Singer ME, Finnerty WR (1990) Physiology of biosurfactant synthesis by *Rhodococcus* sp H13-A. Can J Microbiol 36:741–745
Singh V, Pandey VC, Pathak DC, Agrawal S (2012) Purification and characterization of *Laceyella sacchari* strain B42 xylanase and its potential for pulp biobleaching. Afr J Microbiol Res 6(7):1397–1410
Singleton DR, Dickey AN, Scholl EH, Wright FA, Aitken MD (2016) Complete genome sequence of a bacterium representing a deep uncultivated lineage within the gammaproteobacterial associated with the degradation of polycyclic aromatic hydrocarbons. Genome Announc. https://doi.org/10.1128/genomeA.01086-16
Sophos NA, Vasiliou V (2003) Aldehyde dehydrogenase gene superfamily: the 2002 update. Chem Biol Interact 143–144:5–22
Spain A, Alm E (2003) Implications of microbial heavy metal tolerance in the environment. Rev Undergraduate Res 2:1–6
Streit WR, Schmitz RA (2004) Metagenomics- key to the uncultured microbes. Curr Opin Microbiol 7:492–498
Tabacchioni S, Chiarini L, Bevivino A et al (2000) Bias caused by using different isolation media for assessing the genetic diversity of a natural microbial population. Microb Ecol 40:169–176
Talfournier F, Stines-Chaumeil C, Branlant G (2011) Methylmalonate semialdehyde dehydrogenase from *Bacillus subtilis*: substrate specificity and coenzyme a binding. J Biol Chem 286(25):21971–21981
Tatusov RL, Natale DA, Garkavtsev IV et al (2001) The COG database: new developments in phylogenetic classification of proteins from complete genomes. Nucleic Acids Res 29:22–28
Teal JM, Farrington JW, Burns K, Stegeman J, Tripp BW, Woodin BR, Phinney C (1992) The West Famouth oil spill after 20 years: fate of fuel oil compounds and effects on animals. Marine Pollut Bull 24(12):607–614
Top EM, Springael D (2003) The role of mobile genetic elements in bacterial adaptation to xenobiotic organic compounds. Curr Opin Biotechnol 14:262–269
Trevors JT (1998) Bacterial biodiversity in soil with an emphasis on chemically-contaminated soils. Water Air Soil Pollut 101:45–67
Vasiliou V, Pappa A, Petersen DR (2000) Role of aldehyde dehydrogenases in endogenous and xenobiotic metabolism. Chem Biol Interact 129:1–19
Villadangos AF, Fu H-L, Gil JA, Messens J, Rosen BP, Meteos LM (2012) Efflux permease CgAcr3-1 of *Corynebacterium glutamicum* is an arsenite-specific antiporter. J Biol Chem 287(1):723–735
Vivas A, Moreno B, del Val C, Macci C, Masciandaro G, Benitez E (2008) Metabolic and bacterial diversity in soils historically contaminated by heavy metals and hydrocarbons. J Environ Monit 10:1287–1296
Yakubu MB (2007) Biodegradation of *Lagoma* crude oil using pig dung. Afr J Biotechnol 6(24):2821–2825
Yveline LD, Frederick J, Pierre D, Michael G, Jean CB, Gilbert M (1997) Hydrocarbon balance of a site which had been highly and chronically contaminated by petroleum wastes of refinery from 1956 to 1997. Marine Pollut Bull 22:103–109

Zabielska-Matejuk J, Czaczyk K (2006) Biodegradation of newquartenaey ammonium compounds in treated wood by mould fungi. Wood Sci Technol 40(6):461–475

Zhang D-C, Schinner F, Margesin R (2010a) *Pedobacter bauzanensis* sp. nov., isolated from soil. Int J Syst Evol Microbiol 60:2592–2595

Zhang J, Tang S-K, Zhang Y-Q, Yu L-Y, Klenk H-P, Li W-J (2010b) *Laceyella tengchongensis* sp. nov., a thermophile isolated from soil of a volcano. Int J Syst Evol Microbiol 60:2226–2230

Zhang D-C. Liu H-C, Zhou Y-G, Schinner F, Mrgesin R (2011) *Pseudomonas bauzanensis* sp. nov., isolated from soil. Int J Syst Evol Microbiol 61:2333–2337